**Journal of Information Systems Engineering and Management**
2026, 11(3s)
e-ISSN: 2468-4376
https://www.jisem-journal.com/

**Research Article**

# Robust Nonlinear Control Based on Artificial Intelligence for Electric Vehicles Under Several Constraints

[1]Mouheb Khaled*, [2]Dr. Kouider Laroussi, [3]Rabhi Abdelhamid
[1]doctoral student in electro-mechanics of Zian Achour University, Laboratory of The Applied and Automation and Industrial Diagnostic- Laadi, University of Djelfa 17000, Djelfa, Algeria.
khaled.mouheb@univ-djelfa.dz
[2]PhD of Zian Achour University, Laboratory of The Applied and Automation and Industrial Diagnostic- Laadi, University of Djelfa 17000, Djelfa, Algeria. e-mail: k.laroussi@univ-djelfa.dz

[3]professor of Laboratory of Modeling Information and Systems, Jules Verne University-Picardie,33 Saint Leu Street,8000, Amiens, France, abdelhamid.rabhi@u-picardie.fr

**ARTICLE INFO**

Received: 26 Feb 2026
Revised: 09 April 2026
Accepted: 20 April 2026
Published: 26 April 2026

**ABSTRACT**

In this paper, we propose a neural network algorithm to eliminate uncertainties caused by dynamic compensators used to linearize permanent magnet synchronous motors for electric vehicle traction. To do this, we propose a speed controller based on an artificial neural network algorithm to approximate the dynamics and correlate the uncertain environmental parameters. We first estimate these uncertainties and use them as inputs to the ANN. We then find an adaptation law to eliminate the uncertainties caused by the compensators. The effectiveness and success of the proposed approach compared to classical controllers in different scenarios of electric vehicle traction are demonstrated by simulations of the adaptive ANN on Matlab/Simulink.

**Keywords:** PMSM, PI controller, Robust, vector control, fuzzy logic, artificial neuron network, electric desired speed

## Introduction

Numerous scientists have proven that vehicles powered by fuel-burning internal combustion engines are the cause of numerous respiratory and carcinogenic diseases, and also air pollution through emissions of nitrogen oxides and carbon dioxide. Electric vehicles, on the other hand, disperse no pollution at all [1,2]. Because they have no exhaust, there is no combustion. But its model is very complex due to its many different parts, such as vehicle dynamics, transmission, and electrical machines [3].

One of the parts of the electric vehicle model is the permanent magnet synchronous motor (*PMSM*) [4], which represents the best option for an electric vehicle drive system given these advantages less maintenance and the simplicity of the mathematical model that will be detailed and discussed in this article [5,6,7]. Nevertheless, the problem of regulating its speed has become a subject of interest for many scientists, as have the limitations of conventional regulators in the face of parametric changes in the permanent magnet synchronous machine model [8].

In this controversy several works have emerged to unravel this type of problem, among these works we can distinguish the nonlinear control method (*CNL*) [10]. Nonlinear control theory deals with nonlinear systems, time-varying or both, and covers a broader class of systems that do not obey the superposition principle. This applies to real-world systems because all real-world control systems are nonlinear and are often governed by nonlinear differential equations. Nonlinear control methods have found applications in various fields such as process control, biomedical engineering, robotics, aircraft

Journal of Information Systems Engineering and Management
2026, 11(3s)
e-ISSN: 2468-4376
https://www.jisem-journal.com/

Research Article

and spacecraft control, electrical machines, electric vehicles, *ABS* system.

The control theory discussed has seen notable advancements in the past twenty years, particularly with the integration of the state feedback linearization technique incorporating input-output decoupling, rooted in field orientation control (*FOC*). The conventional proportional-integral (*PI*) controller is widely employed in speed regulation algorithms and path tracking for permanent magnet synchronous motors (*PMSM*) owing to its straightforwardness and practicality in implementation.

Nevertheless, the conventional *PI* controller is susceptible to variations in parameters and struggles to address issues like overshooting and handling speed disturbances efficiently. Conversely, *fuzzy control*, while not mandating a precise mathematical model, exhibits robustness. It heavily depends on expert knowledge and linguistic formalism, potentially resulting in steady-state inaccuracies. Moreover, predictive control and active disturbance rejection control can enhance the system's dynamic performance, yet their algorithms are intricate and challenging to implement. Traditional *PI* controllers are sensitive to parameter changes [11,12], making them unable to quickly resolve overshoots and disturbances [13]. *Fuzzy control*, on the other hand, is robust and does not require a precise mathematical model [14,15]. However, it relies heavily on expert knowledge and linguistic formalism, which can lead to inaccuracies in steady state. Predictive control and active control by disturbance rejection can improve dynamic system performance, but their algorithms are complex and difficult to implement quickly. nonlinear control methods, such as *fuzzy logic* strategy, have been proposed to solve these problems. *fuzzy logic* allows humans to reason by providing an inference structure, and fuzzy logic controllers are simple to conceptualize, consisting of an input stage, a processing stage, and an output stage [16,17]. *fuzzy logic* has been applied to various fields, including longitudinal autopilot attitude control, precision stabilized platforms, and speed tracking systems [18,19].

The second stage after creating the dynamic model is to model the internal components of each subsystem, which will give us a rough idea of the type of control strategy to be used [20,21].

## Modeling Of PMSM

### *A. Mathematical model of PMSM:*

Taking into account the magnetic circuit's non-saturation state and the sinusoidal distributed magneto motive force (*MMF*) produced by the stator windings, the dynamic model of a Permanent Magnet Synchronous Motor (*PMSM*) in a rotor reference frame can be represented by the following equation. [9,38]:

$$[V_{abc}] = [R.\, i_{abs}] + \frac{d[\varphi_{abc}]}{dt} \tag{1}$$

Where:

$$[V_{abc}] = \begin{bmatrix} V_a \\ V_b \\ V_c \end{bmatrix} \quad ; \quad [i_{abs}] = \begin{bmatrix} i_a \\ i_b \\ i_c \end{bmatrix} \tag{2}$$

$$[R] = \begin{bmatrix} R & 0 & 0 \\ 0 & R & 0 \\ 0 & 0 & R \end{bmatrix}$$
$$[\varphi_{abc}] = \begin{bmatrix} \varphi_a \\ \varphi_b \\ \varphi_c \end{bmatrix}; \tag{3}$$

With $V_{abc}$,$i_{abs}$,$\varphi_{abc}$ representing the stator phases 'voltages the stator phases 'currents and the total flux produced by the stator currents. $R$ indicates the resistance of a stator phase.

**Journal of Information Systems Engineering and Management**
2026, 11(3s)
e-ISSN: 2468-4376
https://www.jisem-journal.com/

**Research Article**

*B. Simplification hypothesis:*

Throughout the calculation of the *PMSM* mathematical model in the *d-q* frame, the following assumptions are made [23,24]:

- The absence of saturation in the magnetic circuit.
- The sinusoidal distribution of the *M.M.F* created by the stator windings.
- Hysteresis is negligible with eddy currents and skin effect.
- The notching effect is negligible. The resistance of the windings does not vary with temperature.

Total fluxes are expressed by [24]:

$$[\varphi_{abc}] = [L].[i_{abs}] + [\varphi'_{abc}] \tag{4}$$

$[L] = \begin{bmatrix} L_{ss} & M_s & M_s \\ M_s & L_{ss} & M_s \\ M_s & M_s & L_{ss} \end{bmatrix}$ With:

(5)

$[V_{abc}] = [R].[i_{abs}] + L\frac{d[i_{abs}]}{dt} + \varphi'_{abc}L_{ss}$ and $M_s$ representing the self-inductance and the mutual inductance between stator windings. $\varphi'_{abc}$is the rotor flux seen by the stator winding It represents the amplitudes of the voltages induced in the stator phases without load Substituting (4) in (1) :

(6)

The electromagnetic torque is expressed by [26]:

$$C_{em} = \frac{1}{w_r}[e_{abc}]^t.[i_{abs}] \tag{7}$$

where $e_{abc} = \frac{d\varphi_{abc}}{dt}$ Represents the electromotive force generated by the stator phase. $\omega_r$ is the speed of the rotor in $[rad/s]$. Note that system (4) leads to correlated and strongly nonlinear equations. To simplify this problem, most studies in the literature prefer to use Park's transformation, which provides dummy variables denoted *d-q* by transformations applied to real variables (voltage, current, and flux) - the components of the Park's equation are denoted as [23]. From physically, this transformation is interpreted as replacing the stationary windings $(a, b, c)$ with rotating windings $(d, q)$ that rotate with the rotor. This transformation simplifies the dynamic equations of the *AC* motor. The Park transform is defined as follows [24]:

$$[x_{dq0}] = [K_\theta][x_{abc}] \tag{8}$$

Where $x$ can be current, voltage or flux and $\theta$ is the rotor position. $x_{dq}$ represents the direct and quadrature components of the stator variables (voltage, current, flux and inductance). The transformation matrix $K_\theta$ is given by[25]:

$$[K_\theta] = \sqrt{\frac{2}{3}}\begin{bmatrix} \frac{1}{\sqrt{2}} & \cos(\theta) & -\sin(\theta) \\ \frac{1}{\sqrt{2}} & \cos\left(\theta - \frac{2\pi}{3}\right) & -\sin\left(\theta - \frac{2\pi}{3}\right) \\ \frac{1}{\sqrt{2}} & \cos\left(\theta - \frac{4\pi}{3}\right) & -\sin\left(\theta - \frac{4\pi}{3}\right) \end{bmatrix} \tag{9}$$

**Journal of Information Systems Engineering and Management**
2026, 11(3s)
e-ISSN: 2468-4376
https://www.jisem-journal.com/

**Research Article**

The inverse matrix:

$$[K_\theta]^{-1}=\begin{bmatrix} \frac{1}{\sqrt{2}} & \frac{1}{\sqrt{2}} & \frac{1}{\sqrt{2}} \\ \cos(\theta) & \cos\left(\theta-\frac{2\pi}{3}\right) & \cos\left(\theta-\frac{4\pi}{3}\right) \\ -\sin(\theta) & -\sin\left(\theta-\frac{2\pi}{3}\right) & -\sin\left(\theta-\frac{4\pi}{3}\right) \end{bmatrix} \quad (10)$$

Applying the transformation (8) to the system (1), we have the electrical equations in the ($d$-$q$) reference [21,22]:

$$V_d = R_s.i_d + L_d\frac{d\varphi_d}{dt} - \omega.\varphi_q \quad (11)$$

$$V_q = R_s.i_q + L_q\frac{d\varphi_q}{dt} + \omega.\varphi_d \quad (12)$$

The flux equation [24]:

$$\varphi_d = L_d.i_d + \varphi_f \quad (13)$$

$$\varphi_q = L_q.i_q \quad (14)$$

$\varphi_f$ is the flux created by the magnets in the rotor, By replacing (13) and (14) and in $V_d, V_q$ we obtain the following equations:

$$V_d = R_s.i_d + L_d\frac{di_d}{dt} - P.\omega_r.L_q i_q \quad (15)$$

$$V_q = R_s.i_q + L_q\frac{di_q}{dt} - P.\omega_r.L_d i_d + P.\omega_r.\varphi_f \quad (16)$$

With:

$$\omega = P.\omega_r \quad (17)$$

Electromagnetic torque equation [26]:

$$C_{em} = \frac{3}{2}.P.\left[(L_d + L_q).i_d.i_q + \varphi_f.i_q\right] \quad (18)$$

*C. Field oriented control:*

Utilizing the field-oriented control mechanism with $i_{dref}$=0 [32,33], the expression for electromagnetic torque in to (18) be simplified as follows:

$$\begin{cases} C_{em} = K_e.i_{qref} \\ K_e = \frac{3}{2}.P.\varphi_d = \frac{3}{2}.P.\varphi_f \end{cases} \quad (19)$$

The goal of the control is to create a control law $i_{qref}(t)$ that enables the output (*speed*) to follow the desired reference speed set by the vehicle accelerator pedal. The tracking error $e_{\omega r}(t)$ ($e_{\omega r}(t) \epsilon R$) is defined as:

Journal of Information Systems Engineering and Management
2026, 11(3s)
e-ISSN: 2468-4376
https://www.jisem-journal.com/

Research Article

$$e(t) = \omega_{ref}(t) - \omega_r(t)$$

In the *(d-q)* Park system, the electrical quantities are of the direct current type giving the possibility to make the control similar to the control of direct current machines [27].
The variables $i_d$ and $i_q$ represent the currents along the *d-q* axis, the variables. $V_d$, $V_q$ represent the stator voltages along the *d-q* axis obtained by the Park transformation, $C_{em}$ represents the electromechanical torque of the *PMSM*, $C_r$ represents the resistive torque in our case it is the dynamics of the vehicle, $\omega_r$ represents the mechanical speed of rotation, $\varphi_d, \varphi_q$ Represents the flux along the *d-q* axis:
R: Stator resistance on the referential (*d-q*).
$L_d$ , $L_q$: the inductance on the reference frame (*d-q*).
P: number of pole pairs.
*f*: coefficient of friction.

## Vehicle dynamics

The speed of a vehicle can be expressed as a constant tractive force to be provided as a function of the characteristics of the vehicle (Fig.1), such as: the mass $M_v$ , the rolling friction *f*, its coefficient of penetration in the air $C_x$ and, also on the slope of the road α % of a sum total of the equations of the forces exercised on the vehicle. [29]
The traction force required to move the *EV* is given by the sum of the rolling resistance forces added to the acceleration force $F_{acc}$ [30]. As shown in Fig.1, the rolling resistance forces, detailed by the group of equations (21), are:

- The aerodynamic force $F_{aero}$.
- The force $F_{roul}$ due to the contact of the wheels on the road.
- the gravitational force $F_{gx}$ due to the slope α.

The resistant torque created by the vehicle dynamics is given by the following formula [31]:

$$C_{roul} = F_{trac}.V_{veh} \quad (20)$$

$$\begin{cases} F_{aero} = \rho.\dfrac{(V_{veh-reél})^2}{2}.C_x.S_f \\ F_{roul} = M_v.g.\cos\alpha\,.(C_0 + C_1.V_{veh})^2 \\ F_{gx} = M_v.g.\sin\alpha \\ F_{acc} = M_v.\gamma \end{cases} \quad (21)$$

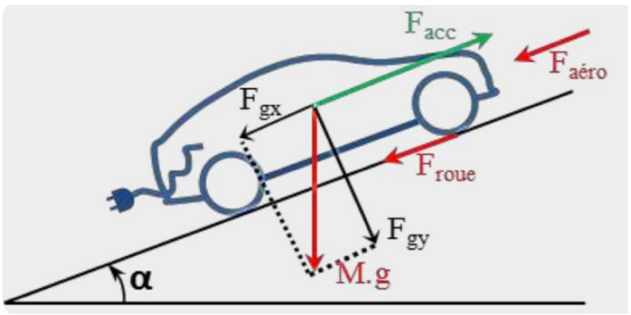


Fig. 1. Forces on a rolling *EV*

**Journal of Information Systems Engineering and Management**
2026, 11(3s)
e-ISSN: 2468-4376
https://www.jisem-journal.com/

**Research Article**

Knowing that:

$$V_{veh-reél} = V_{veh} \pm V_{vent} (22)$$

The force of traction is:

$$F_{trac} = F_{acc} - F_{aero} - F_{roul} - F_{gx} \quad (23)$$

## Structure of the order

To validate the developed model, tests were performed in the *Matlab/Simulink* environment using the parameters shown in Table 1 and 2. The studied system was subjected to various working conditions. Based on the different mathematical laws of the nonlinear control, the control scheme was developed, which combines the two methods (*PI* control and *Fuzzy logic* control) with its controllers for the variable speed drive of the *PMSM* with a mechanical load representing the vehicle dynamics as shown in Fig.2

This block diagram is decomposed in three essential block a block which represents the *PMSM* with its decoupling, controlled by the vector control, the second block represents the dynamics of vehicle which was translated by a torque resistant compared to the *PMSM*, the third block rests on the part control on the speed of rotation which based on the correction of the error

$$e = e_{\omega_r} = (\omega_{ref} - \omega_r) (24)$$

$$de = \frac{de_{\omega_r}}{dt} = \frac{d\omega_{ref}}{dt} - \frac{d\omega_r}{dt} \quad (25)$$

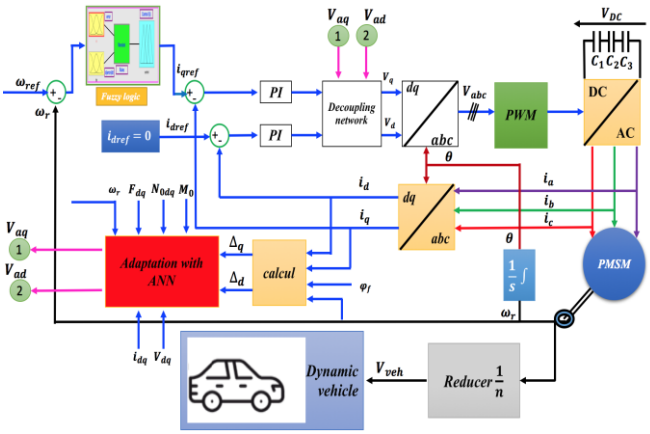


Fig. 2. Block diagram of *PMSM* with adaptation controller

Equations (24) and (25) represent the inputs of the fuzzy logic controller (fig.4). Considering the progress made in normalization.

### *D. PI Regulation:*

In this traditional approach, the Integral Proportional (PI) controller is utilized to rectify the discrepancy between the desired rotational speed and the actual measured rotation speed [32]. In this Controller, the input to the system is the error with constant gain ($K_p$) in addition to the integral of the error e with constant gain ($K_i$) to control the system output $w_r$ as the fig.3. By using the pumping method, we will have the regulator gains as follows: The values of $K_{pw}$ and $K_{iw}$ are respectively 1.735 and 22.5 .By using the decoupling of the vector control, the equation (26) represents the regulation of the currents by the principle of *PI* regulator, for the speed control we will have the equation (27) which gives a reference electromagnetic torque from dynamic rotation speed error

**Journal of Information Systems Engineering and Management**
2026, 11(3s)
e-ISSN: 2468-4376
https://www.jisem-journal.com/

**Research Article**

$$V_{dqr} = K_{pdq}(i_{dqr} - i_{dq}) + \frac{1}{K_{idq}}\int (i_{dqr} - i_{dq}) \quad (26)$$

$$C_{em\_ref} = K_{pw}.(\omega_{ref} - \omega_r) + \frac{1}{K_{iw}}\int (\omega_{ref} - \omega_r) \quad (27)$$

Equations (26) and (27) represent the mathematical formula calculations under the *PI* regulation

*E. Fuzzy logic regulation:*

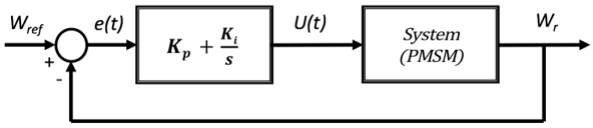


Fig. 3. Functional diagram of a system regulated by the PI regulator

The fuzzy controller employed is of the Mamdani type, structured around a decision-making framework that handles subjective and imprecise rules. The initial stage in developing a fuzzy controller involves selecting its input and output variables, determining the parameters required for the desired outcome, and defining the linguistic ranges of its variables. The system inputs are the error of the angular position ***e*** and its derivative ***de*** (equations (24) and (25). The fuzzy controller is composed:

1. A rule base, which contains the rules describing the expert's conduct.
2. From a decision making logic.
3. A *FUZZIFICATION* interface, which allows transforming the measured input values into measured values into fuzzy values.
4. From a *DEFUZZIFICATION* interface to the output, a precise action is determined from the fuzzy output
5. variables descriptions.

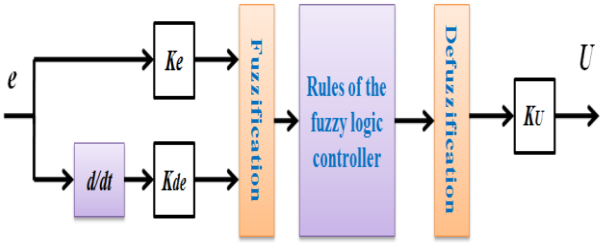


Fig. 4. Functional diagram of a system regulated by the Fuzzy logic controller

Fuzzy logic can deal with situations that are uncertain where the domain knowledge is represented by linguistic variables (SMALL, MEDIUM, LARGE, etc.) with membership values ranging from 0 to 1. Fuzzification, inference, and defuzzification are the three steps of the *FLC* system.

Our study was initiated by establishing fuzzy sets of input and output variables with membership functions of 3, then 5. Comparing the results, we found that the five-set regulator works better.

**Journal of Information Systems Engineering and Management**
2026, 11(3s)
e-ISSN: 2468-4376
https://www.jisem-journal.com/

**Research Article**

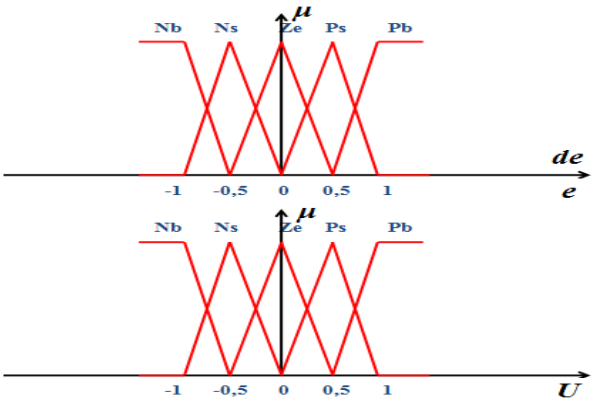


Fig. 5. Membership functions for: input (*e, de*), and output (U) The fuzzy rules are listed in Table 1

The five fuzzy sets that characterize the variables A Mamdani fuzzy logic controller was created with two inputs and one output, each partitioned into five fuzzy sets: Nb (large negative), Ns (small negative), Ze (zero), Ps (small positive), and Pb (large positive). *Gaussian* and *triangular* membership functions were chosen for the inputs and output variables [33]. The Mamdani controller is commonly employed as a feedback controller, establishing a static relationship between the input conditions and the corresponding output actions. This controller mirrors the continuous decision-making process of humans and enables seamless transition between discrete output values. The antecedent and consequent fuzzy sets in Mamdani systems are typically triangular or Gaussian, with input membership functions overlapping in a manner that ensures the membership values of the rule antecedents always sum to one. This design choice allows for a smooth transition between discrete outputs, capturing the continuous nature of human decision-making processes. Mamdani fuzzy inference systems are well suited to expert systems applications where rules are created from human expert knowledge, such as medical diagnoses. The inference process of a Mamdani system involves combining the output fuzzy sets into a single fuzzy set using the FIS aggregation method, then defuzzification the combined output fuzzy set to calculate a final output value sharp. *Fuzzy-PI* controllers have two inputs and one output. The *Fuzzy-PI* controller in Figure 2 is developed using input membership functions for the error e and the change in error of and output membership function for $W_r$, the measured velocity for *PMSM*. [32]
During the simulation of the system with the fuzzy logic control technique, the toolbox rules are shown in Figure 3 and 4, which characterize the correction of the error (***e***) and the variation of the error (***de***) of in the interval [-1 1]. The normalization gains "$K_e$" and "$K_{de}$" " for the committed error and the control gain "$K_U$" " for converting the output were added. [33]
The rules of the five-set fuzzy controller is shown in Table 1 [39]:

TABLE I
RULES OF THE FUZZY LOGIC CONTROLLER

| de / e | Nb | Ns | Ze | Ps | Pb |
|---|---|---|---|---|---|
| Nb | Nb | Nb | Ns | Ze | Ze |
| Ns | Nb | Ns | Ze | Ze | Ze |
| Ze | Ns | Ze | Ze | Ze | Ze |
| Ps | Ns | Ze | Ze | Ps | Ps |
| Pb | Ze | Ze | Ps | Pb | Pb |

**Journal of Information Systems Engineering and Management**
2026, 11(3s)
e-ISSN: 2468-4376
https://www.jisem-journal.com/

**Research Article**

### *F. Neural Network Controller*

The utilized neural network features a single hidden layer consisting of eight neurons, with the activation functions "*tansig*" and "*purelin*"[34]. The Levenberg-Marquardt algorithm was employed for learning in order to achieve optimal results [34]. Once the network structure was determined, the optimization of connection weights, also known as the learning process, could commence. The structure of the network significantly impacts the learning process and the quality of control, as the approximation error depends on both the number of neurons in the hidden layer and the information input to the network [35].

Mathematically developing the equations of the machine. We have:

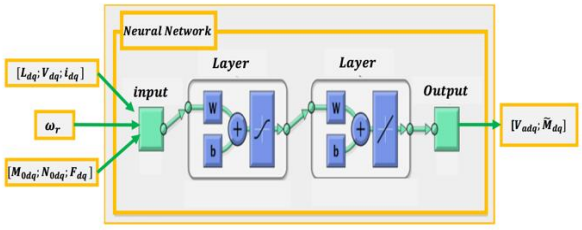


Fig. 6. Type of neural network used

$$\begin{cases} L_d.\frac{di_d}{dt} = V_d - R_s.i_d + P.\omega_r.L_q.i_q \\ L_q.\frac{di_q}{dt} = V_q - R_s.i_q - P.\omega_r.L_d i_d - P.\omega_r.\varphi_f \end{cases} \quad (28)$$

Equation (28) becomes:

$$\begin{cases} V_d = R_s.i_d + L_d\frac{di_d}{dt} - P.\omega_r.L_q.i_q \\ V_q = R_s.i_q + L_q\frac{di_q}{dt} + P.\omega_r.L_d i_d + P.\omega_r.\varphi_f \end{cases} \quad 29)$$

According to the equations (29) we obtain:

$$\begin{cases} \frac{di_d}{dt} = \frac{V_d - R_s.i_d}{L_d} + \frac{(P.\omega_r.L_q.i_q)}{L_d} \\ \frac{di_q}{dt} = \frac{V_q - R_s.i_q}{L_q} + \frac{(-P.\omega_r.L_d i_d - P.\omega_r.\varphi_f)}{L_q} \end{cases} (30)$$

We want to write the system of equation (30) in the following form in (31):

$$\begin{cases} \frac{di_d}{dt} = \frac{U_d}{L_d} + \Delta_d \\ \frac{di_q}{dt} = \frac{U_q}{L_q} + \Delta_q \end{cases} \quad (31)$$

The resulting errors are caused by parametric and driving cycle uncertainties imposed on the electric vehicle (reference speed $\omega_{ref}$) therefore to improve the performance of the permanent magnet synchronous machine(*PMSM*), two adaptive blocks using artificial neural networks (*ANN*) were used

**Journal of Information Systems Engineering and Management**
2026, 11(3s)
e-ISSN: 2468-4376
https://www.jisem-journal.com/

**Research Article**

to reinforce the system with machine equations for targeted errors $\Delta_d$ and $\Delta_q$.Since the controlled system is decoupled into two subsystems, we develop the *ANN* using two pairs "input /output", namely:

- the d-system: p=$[V_d, i_d]$,and $\Delta_d$ as target vector.
- the q-system: p=$[V_q, \omega_r]$,and $\Delta_q$ as target vector.

Therefore, the deduced from equations (30) and (31) gives the following expressions for $\Delta_d$ and $\Delta_q$

$$\begin{cases} \Delta_d = \dfrac{(P.\omega_r.L_q.i_q)}{L_d} \\ \Delta_q = \dfrac{(-P.\omega_r.L_d i_d - P.\omega_r.\varphi_f)}{L_q} \end{cases} \tag{32}$$

### G. *Control using Neural Networks with Fuzzy Regulators*

Once the learning phase has been completed, we turn to the implementation under *Matlab/Simulink* of two neural blocks allowing us to estimate the adaptive terms "$V_{ad}$" and "$V_{aq}$" (Fig.7) which will aim to compensate for the targeted disturbance terms $\Delta_d$ and $\Delta_q$.

The adaptive terms $V_{ad}$ and $V_{aq}$ gives the possibility to adjust the high uncertainties $\Delta_d$ and $\Delta_q$.$V_{ad}$ and $V_{aq}$ are calculated using the following formulas[36]:

$$\begin{cases} V_{ad} = \dot{\hat{M}}^T \sigma(N_0^T \mu_d) \\ V_{aq} = \dot{\hat{M}}^T \sigma(N_0^T \mu_q) \end{cases} \tag{33}$$

With:

$$\begin{cases} \mu_d = [V_d \; i_d]^T \\ \mu_q = [V_q \; \omega_r]^T \end{cases} \tag{34}$$

The estimate of M, denoted as $\dot{\hat{M}}$, is updated according to the following adaptation law [36,37]:

$$\dot{\hat{M}} = -F_{aq}\left[2\left(\sigma N_0^T \mu_{aq}\right).\widetilde{\iota_{aq}} + K_{aq}\left(\hat{M} - M_0\right)\right] \tag{35}$$

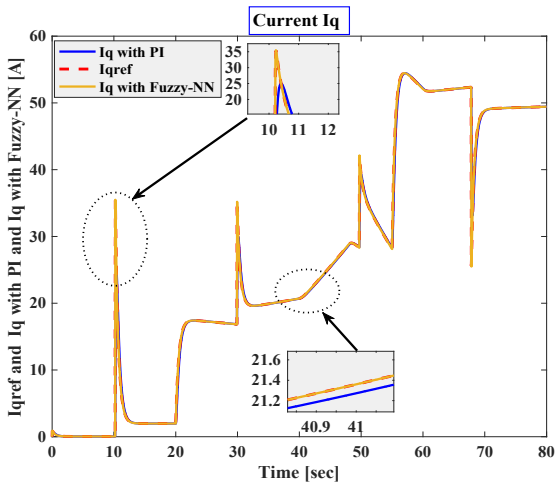


Fig. 10. variation of current $I_q$

**Journal of Information Systems Engineering and Management**
2026, 11(3s)
e-ISSN: 2468-4376
https://www.jisem-journal.com/

**Research Article**

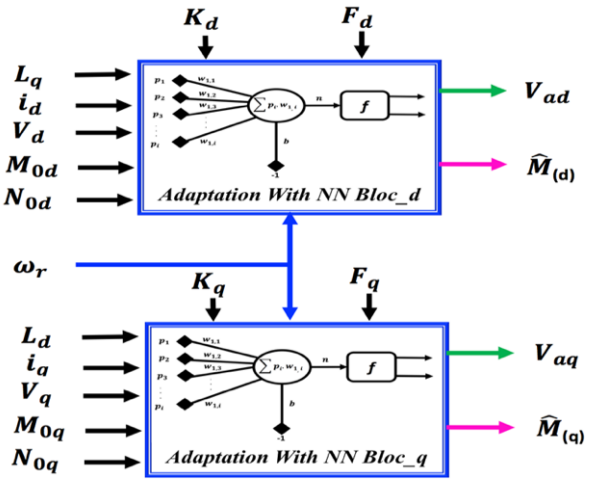


Fig. 7. Adaptive control with neural networks (NN)

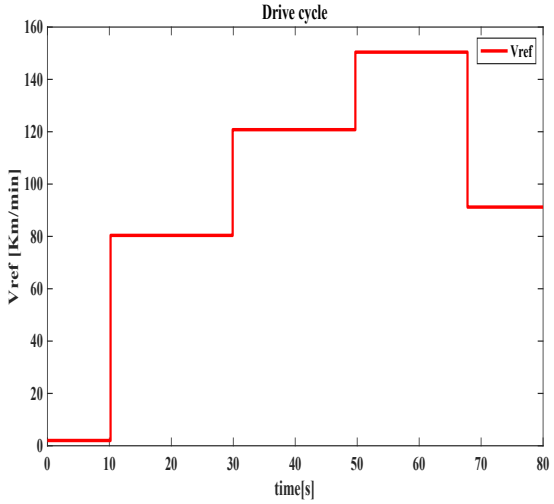


Fig.8. Drive cycle of speed

## RESULTS AND DISCUSSION

After subjecting the control system to different working conditions: regulation *PI*, then the second test by the fuzzy neural network control, we obtained the following results:

**Journal of Information Systems Engineering and Management**
2026, 11(3s)
e-ISSN: 2468-4376
https://www.jisem-journal.com/

**Research Article**

*H. Drive cycle of speed:*

The results of the electric vehicle simulation under Matlab/Simulink are illustrated as follows:

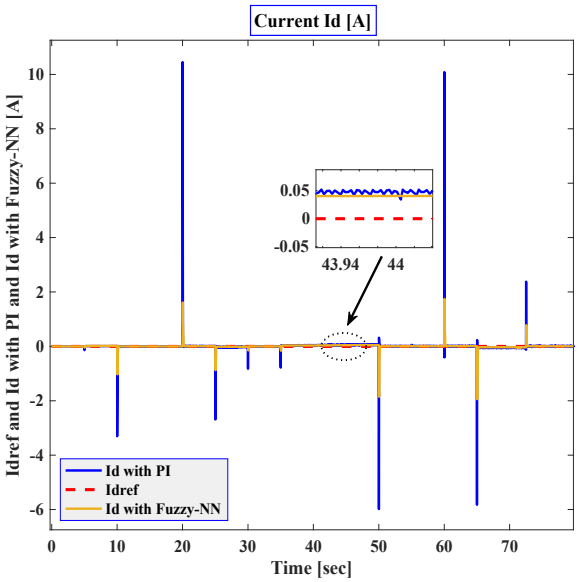


Fig. 9. variation of current $I_d$

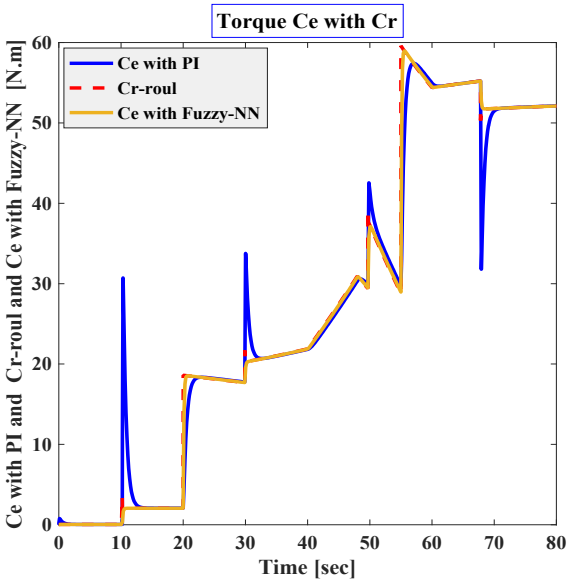


Fig. 11. variation of torque $C_{r\text{-}roul}$ and $C_e$ with *PI* and $C_e$ with *Fuzzy-NN*

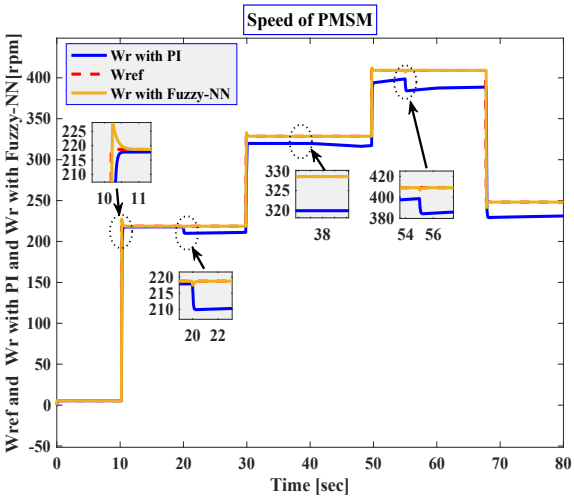


Fig. 12. speed of rotation $W_r$

The Fig.9. represents the variation of the current of the synchronous motor $I_d$ with permanent magnet as a function of time, according to the two control strategies (*PI* controller and network regulator of fuzzy neurons), and, we note that the current has peaks author of its reference ($i_{dref}$= 0) which are caused by the variation of the speed and the errors of the modeling. Comparing between the two PI results and with fuzzy reinforced by artificial neural networks, we see that the response obtained by the *Fuzzy-NN* regulator is closer to the record than that obtained by the *PI* regulator. The current regulation generates in this case the optimization of the energy consumed by the applied control, a good decoupling of the vector control *FOC*.

Fig.10. shows the variation in the current $I_q$ of the synchronous permanent magnet motor as a

**Journal of Information Systems Engineering and Management**
2026, 11(3s)
e-ISSN: 2468-4376
https://www.jisem-journal.com/

**Research Article**

function of time, according to the two control strategies (*PI* and fuzzy logic reinforced by the adaptation *ANN*) we note that the current obtained by the PI regulator ($I_q$ with *PI*) is almost identical to that obtained by the fuzzy-NN regulator ($I_q$ with Fuzzy-NN) and by a zoom on the range of Matlab, we see a small difference which can be the cause of the comparison between the two commands before the reference. The two strategies are therefore effective for regulating the current, in terms of precision the choice is the *Fuzzy-NN* command. And by a zoom in the range of Matlab we see a small difference which can be the cause of the comparison between the two commands before the reference. The two strategies are therefore effective for regulating the current, in terms of precision the choice is the *Fuzzy-NN* command. The two strategies are therefore effective for regulating the current, in terms of precision the choice is the *Fuzzy-NN* command.

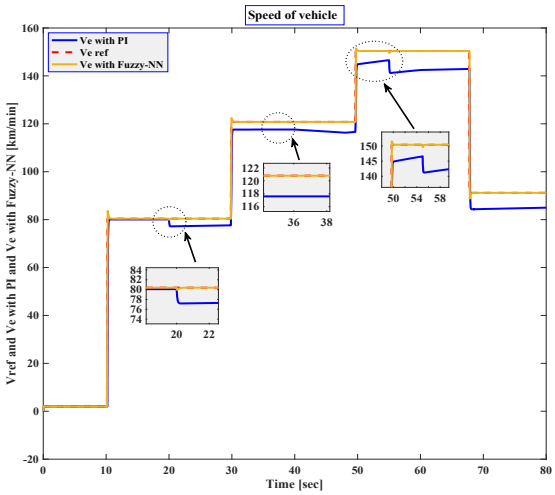


Fig. 13. speed of the vehicle $V_e$

Fig.11 shows the variation of the electromagnetic torque and the resisting torque created by the dynamics of the vehicle on the electric motor as a function of the time which varies between 0 *sec* and 80 *sec*. The two results are good compared to the stress applied to the ($C_e$ engine with *PI* and $C_e$ with *Fuzzy-NN*) but by direct observation we notice that the torque with $C_e$ with *Fuzzy-NN* is closer to the set point and follows the resistant couple $C_{r\text{-}roul}$. The torque being varied as a function of time to follow the variation of the resistant torque with small errors caused by the variation of the slope and the variations of the parameters inside the motor against $C_e$ with *PI* does not follow the resistant couple well, lack of precision.

Fig.12 shows the rotation speed of the synchronous motor as a function of time [0 *sec* to 80 *sec*] with the reference speed, by both techniques ($W_r$ with PI and $W_r$ with *Fuzzy-NN*) We observe a good continuation of the instructions by the adaptive fuzzy regulation based on artificial neural networks compared to the *PI* regulator. On the other hand, in the *PI* controller, we note the absence of reference tracking caused by the parametric change of the stator resistance *R* and the stator inductance *L*. This variation generates the malfunction of the vector control *FOC*. In this case, precision is a factor that plays an essential role in our system to ensure the proper monitoring and stability of the system. A p% slope at time (20s) of 20° shows the robustness of the control by the zoom of this moment, the same test at time (60s) with an increase of 45°,the zoom at time 60 s indicates the response of the system, so the correct reference follows-The model obtained by the fuzzy regulator reinforced by artificial neural networks. This control is a proof of robustness in the face of parametric change and external uncertainties (applied slope on the trajectory) and in front of the imposed drive cycle.

Fig.13 shows the variation in vehicle speed as a function of time from 0 s to 80 s. This speed is the result of the rotation speed of the *PMSM* multiplied by the transformation gain in this case where we observe the response obtained by the two strategies ( *PI* and *Fuzzy-NN*), the speed obtained by the PI

($V_e$-*PI*) regulator having deviations with its reference ( Zoom at time 36s ), which shows the absence of the pursuit, while the *Fuzzy-NN* regulation satisfies this pursuit between the measured value $V_e$ *with Fuzzy-NN)* and the speed reference ($V_{ref}$) the performance of this vehicle improves in terms of speed in the case of an adaptive fuzz regulator in terms of tension with neural networks

## Conclusion

The automaton with fuzzy logic reinforced by an artificial adaptation proves much more robust because the speed of the motor makes it possible to follow much more quickly the reference rotation speed in the case of a change abrupt and in relation to external disturbances, on the other hand the results obtained by the classic regulation ( *PI* regulator ) have overshoots concerning the motor torque so the most robust and effective control among these two techniques is the fuzzy control adaptive logic. From the point of view of this work, the control of adaptive fuzzy logic in voltage is effective in the case of changes in parameters of the electric motor, but it lacks sensitivity to engine uncertainty at this stage, the system must improve the target error and external disturbances caused by the environment, the major drawback of the control requires a data and additional information.

Therefore, our system needs adaptive predictive control to improve performance, stability and reference tracking; in the future we will be interested in adaptive predictive control

## References

[1] Bouguenna, Ibrahim Farouk, et al. "Robust neuro-fuzzy sliding mode control with extended state observer for an electric drive system." Energy 169 (2019): 1054-1063. J. Clerk Maxwell, A Treatise on Electricity and Magnetism, 3rd ed., vol. 2. Oxford: Clarendon, 1892, pp.68–73.
[2] Gnap, Jozef, et al. "The impact of road transport on the environment." Ecology in Transport: Problems and Solutions (2020): 251-309.
[3] Ju, Zhiyang, et al. "A survey on attack detection and resilience for connected and automated vehicles: From vehicle dynamics and control perspective." IEEE Transactions on Intelligent Vehicles (2022).
[4] Zhang, Yunfei, et al. "Dynamic simulation of permanent magnet synchronous motor (PMSM) electric vehicle based on Simulink." Energies 15.3 (2022): 1134.
[5] Ibrahim, Amier, and Fangming Jiang. "The electric vehicle energy management: An overview of the energy system and related modeling and simulation." Renewable and Sustainable Energy Reviews 144 (2021): 111049.
[6] İnci, Mustafa, et al. "A review and research on fuel cell electric vehicles: Topologies, power electronic converters, energy management methods, technical challenges, marketing and future aspects." Renewable and Sustainable Energy Reviews 137 (2021): 110648.
[7] Usman, Adil, Nikhil T. Doiphode, and Bharat S. Rajpurohit. "Finite element modeling of stator winding faults in permanent magnet synchronous motor: Part II." 2019 International Conference on Electrical Drives & Power Electronics (EDPE). IEEE, 2019.
[8] Künzler, Moritz, et al. "Dimensioning of a permanent magnet synchronous machine for electric vehicles according to performance and integration requirements." Automotive and Engine Technology 7.1-2 (2022): 97-104.
[9] Feng, W., Bai, J., Zhang, Z., & Zhang, J. (2022). A Composite Variable Structure PI Controller for Sensorless Speed Control Systems of IPMSM. Energies, 15(21), 8292.
[10] Zhu, Y., Wang, Z., Guo, X., & Wei, Z. (2023). An improved kinetic energy control strategy for power smoothing of PMSG-WECS based on low pass filter and fuzzy logic controller. Electric Power Systems Research, 214, 108816.
[11] Lin, R.; Chen, S.; Ding, X. Modélisation et simulation du contrôle PID à séparation intégrale des neurones pour moteur synchrone à aimant permanent. J. Fuzhou Univ. 2009 , 37 , 849–852.

[12] Ding, W.; Gao, L. Modélisation et simulation d'un système de contrôle vectoriel de moteur synchrone à aimant permanent. Micromoteurs 2010 , 43 , 66–71
[13] Chen, Z.; Zhang, ZH Stratégie de découplage du courant et de suppression des harmoniques du moteur synchrone à aimant permanent basée sur le contrôle proportionnel du rejet des perturbations actives à résonance. Proc. SCEE 2021 , 58 , 1–10.
[14] Sha, L.; Chanson, Y. ; Li, Z. Méthode de contrôle de moteur synchrone à aimant permanent basée sur un PI flou et un observateur en mode glissant. J.Phys. Conf. Ser. IOP Publ. 2022 , 2218 , 012053.
[15] Ding, X.; Li, R.; Cheng, Y.; Liu, Q. ; Liu, J. Conception et recherche d'un système de contrôle de suspension PID à plusieurs flous basé sur la reconnaissance de la route. Processus 2021 , 9 , 2190.
[16] Wang, AP ; Huang, XZ Modèle à coefficient de poids variable Méthode de contrôle de courant prédictif pour moteur synchrone linéaire à aimant permanent. Proc. SCEE 2022 , 59 , 1–11.
[17] Yang, PM ; Liu, Stratégie de contrôle de la stabilité de la tension YC basée sur la compensation de courant prédictive du modèle. Micromoteurs 2022 , 55 , 56–64.
[18] Bai, CG ; Wei, XJ Research on Nonlinear Active Disturbance Rejection Compound Control Strategy of Permanent Magnet Synchronous Motor. Petite spécification. Électr. Mach. 2021 , 49 , 46–50.
[19] Ferdinando Luigi Mapelli, Davide Tarsitano, and Marco Mauri. Plugin hybrid electric vehicle : Modeling, prototype realization, and inverter losses reduction analysis. IEEE Transactions on Industrial electronics, 57(2) :598–607, 2010.
[20] Ghezouani, Abdelkader, et al. "Comparative study of pi and fuzzy logic based speed controllers of an ev with four in-wheel induction motors drive." *Journal of Automation Mobile Robotics and Intelligent Systems* 12 (2018).
[21] Naikawadi, Komal, et al. "Inductance Estimation of PMSM Using Extended Kalman Filter." Int. J. Electr. Electron. Res 11 (2023): 138-142.
[22] Yuan, Tianqing, et al. "Improved H∞ repetitive controller for current harmonics suppression of PMSM control system." Energy Reports 8 (2022): 206-213.
[23] Sarsembayev, Bayandy, Kanat Suleimenov, and Ton Duc Do. "High order disturbance observer based PI-PI control system with tracking anti-windup technique for improvement of transient performance of PMSM." IEEE Access 9 (2021): 66323-66334.
[24] Iturra, R. Guzman, and P. Thiemann. "Sensorless Field Oriented Control of PMSM using Direct Flux Control with improved measurement sequence." 2021 XVIII International Scientific Technical Conference Alternating Current Electric Drives (ACED). IEEE, 2021.
[25] Wang, Qiong, Shuanghong Wang, and Chuanhai Chen. "Review of sensorless control techniques for PMSM drives." IEEJ Transactions on electrical and electronic engineering 14.10 (2019): 1543-1552.
[26] Kulkarni, Sandhya, and Archana Thosar. "Performance analysis of fault tolerant operation of PMSM using direct torque control and fuzzy logic control." IJEER 10.2 (2022): 297-307.
[27] Aymen, Flah, et al. "Electric vehicle model based on multiple recharge system and a particular traction motor conception." IEEE Access 9 (2021): 49308-49324.
[28] Rauth, Sheshadri Shekhar, and Banshidhari Samanta. "Comparative analysis of IM/BLDC/PMSM drives for electric vehicle traction applications using ANN-based FOC." 2020 IEEE 17th India Council International Conference (INDICON). IEEE, 2020.
[29] Peng, Jeffrey, et al. "Influence of translational vehicle dynamics on heavy vehicle noise emission." Science of the Total Environment 689 (2019): 1358-1369.
[30] Al Halabi, Marah, and Anas Al Tarabsheh. Modelling of electric vehicles using Matlab/Simulink. No. 2020-01-5086. SAE Technical Paper, 2020.
[31] Tahouni, Amin, Mehdi Mirzaei, and Behrouz Najjari. "Novel constrained nonlinear control of vehicle dynamics using integrated active torque vectoring and electronic stability control." IEEE Transactions on Vehicular Technology 68.10 (2019): 9564-9572.
[32] Li, Hu, et al. "Adaptive fuzzy PI controller for permanent magnet synchronous motor drive based on predictive functional control." *Journal of the Franklin Institute* 358.15 (2021): 7333-7364.

[33] HAMOU, Ait Abbas, KHALED, Mouheb, CYLIA, Aliouat, et *al.*Comparative study of the intelligent techniques (fuzzy logic and neural network) of the ABS system. In : *2022 19th International Multi-Conference on Systems, Signals & Devices (SSD)*. IEEE, 2022. p. 1497-1503.

[34] Sharma, Ujjwal, Nakul Gupta, and Manvendra Verma. "Prediction of the compressive strength of Flyash and GGBS incorporated geopolymer concrete using artificial neural network." Asian Journal of Civil Engineering (2023): 1-14.

[35] Ait Abbas, H., Belkheiri, M and Zegnini, B. (2015a) 'Feedback linearization control for highly uncertain nonlinear systems augmented by SHL NNs', *Journal of Engineering Science and Technology Review*, Vol. 8, No. 2, pp.215-224.

[36] Ait Abbas, H., Belkheiri, M and Zegnini, B. (2016) 'Feedback linearization control of an induction machine augmented by SHL NNs', *International Journal of Control*, Vol. 89, No. 1, pp.140-155, doi:10.1080/00207179.20151063162.

[37] Zhou, Sihui, Yongming Li, and Shaocheng Tong. "Finite-time adaptive neural network event-triggered output feedback control for PMSMs." Neurocomputing 533 (2023): 10-21.

[38] Velarde-Gomez, Sergio, and Eduardo Giraldo. "Robust State Space Embedded Control of a 3D Printed Permanent Magnet Synchronous Motor." *IAENG International Journal of Applied Mathematics* 54.2 (2024).

[39] Wei, Yuan, et al. "Driving Path Tracking Strategy of Humanoid Robot Based on Improved Pure Tracking Algorithm." *IAENG International Journal of Applied Mathematics* 54.2 (2024).